Pressureless Euler equations with maximal density constraint : a time-splitting scheme

Bertrand Maury, Anthony Preux

B. Maury and A. Preux

Pressureless Euler equations with maximal density constraint : a time-splitting scheme

Abstract: In this paper, we consider the pressureless Euler equations with a congestion constraint. This system still raises many open questions and, aside from its one-dimensional version, very few is known concerning its solutions. The strategy that we propose relies on previous works on crowd motion models with congestion in the framework of the Wasserstein space, and on a microscopic granular model with nonelastic collisions. We illustrate the approach by preliminary numerical simulations in the two-dimensional setting.

Keywords: Pressureless Euler equations, congestion, optimal transportation.

1 Introduction

We are interested in the pressureless gas dynamics system, that describes the free motion of inertial particles. The system simply expresses mass conservation and momentum conservation:

$$\begin{cases} \partial_t \rho + \partial_x(\rho u) = 0 \\ \partial_t(\rho u) + \partial_x(\rho u^2) = 0. \end{cases} \tag{1}$$

Here, ρ represents the density of particles and u is the velocity field. The fact that a single velocity can be locally defined is a strong implicit assumption here. The real free transport equation for non-interacting particles would be of the kinetic type (namely the Collisionless Boltzmann equation), allowing for various velocities to coexist at the same place. In the previous system (1), even for smooth initial data, transport characteristics are likely to cross, leading to an incompatibility in terms of velocity. Preserving the monokinetic character of the

B. Maury: Laboratoire de Mathématiques d'Orsay, Univ. Paris-Sud, CNRS, Université Paris-Saclay, 91405 Orsay, France & DMA, École Normale Supérieure, 45 rue d'Ulm, Paris
A. Preux: Laboratoire de Mathématiques d'Orsay, Univ. Paris-Sud, CNRS, Université Paris-Saclay, 91405 Orsay, France

representation calls for considering interactions between particles, although they do not explicitly appear in the equation.

As described on [1] or [2], this model can create Dirac Masses even if initial data are smooth. It is therefore necessary to define measure-valued solutions for this system. The existence of such solutions of (1) has been proven constructively in [3] and [4], by approximating the initial measure by Dirac masses (sticky particles). The motion of the corresponding collection of particles is then computed, following an event-driven approach to handle binary collisions, and the corresponding sticky particle solutions are shown to converge as the number of particles tends to infinity. This approach has been introduced in [5] as a model describing the formation of galaxies in the early stage of the universe. This system has been studied in the framework of hyperbolic systems of conservation laws (see for instance [6] and [7]), although it lacks hyperbolicity. A proof of uniqueness has been given in [8] with appropriate conditions on entropy and energy. This system has also been formulated and analyzed as a first order differential inclusion, see [9, 10]. Some other approaches have been proposed, for instance, in [11] with an optimal transportation approach, with a viscosity regularization in [12] and [13], with finite size sticky particles in [14].

We are interested here in the situation where the density is subject to remain below a threshold value, say 1; it corresponds to the pressureless gas dynamics with congestion constraint :

$$\begin{cases} \partial_t \rho + \partial_x(\rho u) = 0 \\ \partial_t(\rho u) + \partial_x(\rho u^2 + \pi) = 0 \\ \rho \leq 1 \\ (1-\rho)\pi = 0 \\ \pi \geq 0. \end{cases} \tag{2}$$

A first approach and numerical algorithm have been given in [15], and the existence of solutions is proved in [16]. The approach is constructive, and dedicated to the one-dimensional setting: it is based on a generalization of the sticky particles model. Particles have been replaced by macroscopic congested blocks, but the dynamic is similar, with a pressure π that is active in congested zone only (a typical collision between two identical blocks is represented in Fig. 1 (top)). In [17] a similar system is obtained and analysed as a limit of the Aw-Rascle model.

Both systems (1) and (2) admit infinitely many solutions, some of them being highly non-physical. Consider for example the case without congestion (1), and ρ defined as follows: ρ is a Dirac mass at 0 during $[0, 1]$, and splits at time 1 into two half Dirac masses, one going to the right at constant velocity u, and

the other one at velocity $-u$, where $u > 0$ is arbitrary. This measure path, with its obvious associated velocity, verifies the system although it does not correspond to any physical reality. The fact that such solutions are compatible with (1), although no interaction force explicitly appears, can be explained: a Dirac mass can be considered as the sum of two half Dirac masses at the same point. Splitting is achieved by exerting an impulsion of one of the halves, and the opposite impulsion on the other. Since these impulsions sum up to zero, it can be done without any real action on the system, and the obtained path verifies the weak formulation of the system. The splitting time is of course arbitrary, and each of the subparticles can be further split in lighter particles, at any time, as soon as local conservation of mass and momentum are respected. Similar *bizarre* solutions can be built for the congested case. An initially steady block can be suddenly splits in two halves, with a pressure field that is singular in time, but regular in space at the instant of the splitting (piecewise affine function vanishing at the ends of the block, maximal at the center). One may hope to recover uniqueness by demanding that the kinetic energy decreases. This is not enough, as the following example shows: consider two Dirac masses heading to 0 with opposite velocities u and $-u$. They may collide at 0 into a steady Dirac mass with weight 2, but they may also bounce against each other, and head back to $-\infty$ and $+\infty$ at velocities $-eu$ and eu, respectively. For any $e \in [0,1]$ (restitution coefficient), the solution is energy decreasing (with conservation for the purely elastic case $e = 1$).

To sum up, both systems allow for multiple solutions to exist, some of them being non-physical (energy increasing). But still infinitely many energy-decreasing solutions exist. A collision law is obviously lacking. Before writing the multidimensional version of (2), let us describe now the two main ingredients that we will use to write the model (with a collision law) and to elaborate a time-splitting strategy.

First ingredient: microscopic granular model

At the microscopic level, the motion of rigid particles can be modelled as follows. Consider N rigid spheres in $\mathbb{R}^d$, with common radius $r > 0$, unit mass, and centers $q_1, \ldots, q_N$. Denote by $q \in \mathbb{R}^{dN}$ the vector of positions, and let $D_{ij} = |q_j - q_i| - r$ denote the inter-grain distance. Prescribing grain rigidity amounts to define a set of feasible configurations, that is

$$\tilde{K} = \left\{ q = (q_1, \ldots, q_N) \in \mathbb{R}^{dN} \ , \ \ D_{ij} \geq 0 \quad \forall i \neq j \right\}.$$

The cone of feasible velocities (i.e. velocities that do not lead to overlapping between grains) is defined for any $q \in \tilde{K}$ as

$$C_{\tilde{K}}(q) = \{v \in \mathbb{R}^{dN} \ , \ \ D_{ij} = 0 \Longrightarrow G_{ij} \cdot v \geq 0\},$$

where $G_{ij} \in \mathbb{R}^{dN}$ is the gradient of D_{ij}. The inertial motion of this system of grains submitted to a force field f (possibly including interactions, i.e. f may depend on q) with nonelastic collision can be written (see e.g. [18, 19])

$$\begin{cases} dq/dt = u \\ du/dt = f + \displaystyle\sum_{i<j} \pi_{ij} G_{ij} \\ \\ q \in \tilde{K} \\ \pi_{ij} D_{ij} = 0 \quad \forall i,j \\ \pi_{ij} \geq 0 \quad \forall i,j \\ u^+ = \mathbb{P}_{C_{\tilde{K}}(q)}(u^-). \end{cases} \tag{3}$$

The π_{ij}'s play the role of a discrete pressure, that is a Lagrange multiplier associated to the non-overlapping constraint $q \in \tilde{K}$. Velocities u^+ and u^- are pre- and post-collisional velocities (as detailed in [19], the velocity has bounded variation, so that left and right limits are well-defined). Note that, when there is no contact, all the distances D_{ij} are positive, so that $\pi_{ij} \equiv 0$, $C_{\tilde{K}}(q) = \mathbb{R}^{dN}$, and we recover the usual Newton law for a N-particle system. The interaction forces π_{ij} are actually measures in time, and they are indeed singular as soon as a collision happens.

Existence of solutions to this system is proved in [18, 19]. Note that, although the system is formally well-posed (uniqueness holds when the number of collision is bounded), uniqueness requires analiticity of the forcing term f (see in particular [18]).

Remark 1. *Let us remark that alternative collisions laws may be accounted for (we shall not extend this generalization to the macroscopic setting) by introducing the so called outward normal cone to K, that is*

$$N_{\tilde{K}}(q) = C_q^\circ = \left\{v \in \mathbb{R}^{dN} \ , \ \ v \cdot w \leq 0 \quad \forall w \in C_{\tilde{K}}(q)\right\}$$

$$= \left\{ v = -\sum_{i<j} \pi_{ij} G_{ij} \ , \ \ \pi_{ij} \geq 0 \ , \ \ D_{ij}\pi_{ij} = 0 \right\}.$$

Given a restitution coefficient $e \in [0,1]$ ($e = 0$ for non elastic shocks and $e = 1$ for purely elastic shocks), a more general collision law is (see e.g. [18])

$$u^+ = u^- - (1+e)\mathbb{P}_{N_{\tilde{K}}(q)}(u^-). \tag{4}$$

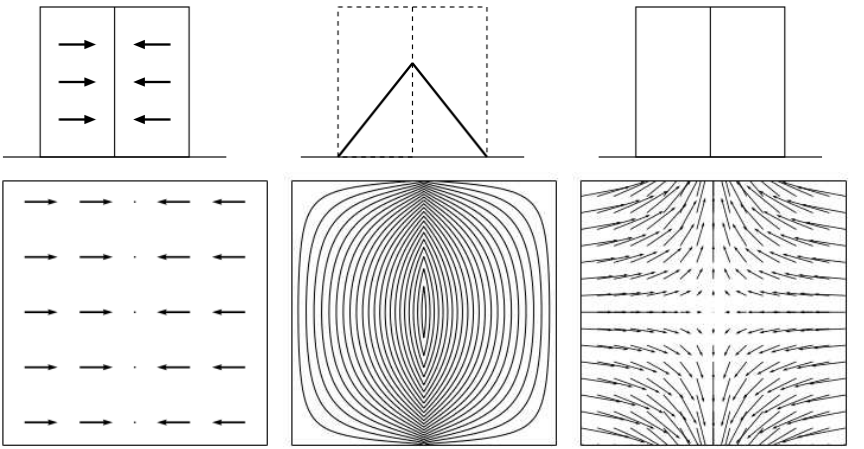

Fig. 1. Collision of two rectangular blocks: pre-collision velocity, instantaneous pressure and post-collision velocity (top: one-dimensional setting; bottom: two-dimensional setting)

Second ingredient: first order crowd motion model

The handling of congestion in evolution equations has been studied for the macroscopic crowd motion introduced in [20] and [21]. The model is based on a so-called *desired* velocity, that is the velocity $U(x)$ someone at x would spontaneously have, if he/she were alone. We aim at accounting for a congestion constraint $\rho \leq 1$, we denote the corresponding set of densities by K. To that purpose, we consider that the desired velocity is projected (in a L^2 sense) on the cone of feasible velocities. The latter set is defined as the set of all those velocities that do not lead to a violation of the constraint. More formally (see [21] for details), it is defined in a dual way :

$$C_K(\rho) = \left\{ v \in L^2 \ , \quad \int v \cdot \nabla q \leq 0 \ , \quad \forall q \in H^1 \ , \quad q \geq 0 \ , \quad q(1-\rho) = 0 \right\}. \tag{5}$$

The model writes

$$\begin{cases} \partial_t \rho + \nabla \cdot (\rho u) = 0 \\ u = \mathbb{P}_{C_K(\rho)}(U). \end{cases} \tag{6}$$

In the spirit of the Catching Up algorithm initially proposed in [22], and applied to a microscopic crowd motion model in [23], a time-stepping algorithm has been proposed in [20] to handle this type of evolution problem. It simply consists in transporting the density during one time step with the desired velocity, possibly violating the constraint, and then project in the Wasserstein sense in the set K

of admissible densities. It reads as follows :

$$\begin{cases} \tilde{\rho}^{n+1} = (\mathrm{Id} + \tau U)_{\#}\rho^n \\ \rho^{n+1} = \mathbb{P}_K^{\mathcal{W}_2}(\tilde{\rho}^{n+1}). \end{cases} \tag{7}$$

Now let us expand System (2) in higher space dimension, with the continuous counterpart of a non-elastic collision law:

$$\begin{cases} \partial_t \rho + \nabla \cdot (\rho u) = 0 \\ \partial_t(\rho u) + \nabla \cdot (\rho u \otimes u) + \nabla \pi = 0 \\ \rho \leq 1 \\ (1-\rho)\pi = 0 \\ \pi \geq 0 \\ u^+ = P_{C_K(\rho)}(u^-). \end{cases} \tag{8}$$

In the previous system, π is a nonnegative scalar field that is the continuous counterpart of the interaction pressures $\pi_{ij}{}'s$ accounting for interactions between neighboring grains in the microscopic model. As previously said, in the one-dimensional setting, it is natural and easy to build exact solutions to this system. Let us stress that sticky block solutions described in [16] verify the non-elastic collision law that we added to the system. Such a collision is represented in Fig. 1 (top). See in particular the pressure field π (middle) that is activated at the very instant of impact; its opposite gradient instantaneously anihilates the pre-collisional velocity field.

In higher dimension, such analytical solutions are not available. Consider for instance the two-dimensional counterpart of the 1D sticky blocks: two rectangular blocks colliding with opposite velocities. At the instant of collision, it can be checked that the pressure field π solves a Poisson equation over the two-blocks domain, with a right-hand-side that is the opposite of the divergence of the pre-collisional velocity (it is a singular distribution supported by the interface), and with homogeneous Dirichlet boundary conditions on the exterior boundary. The corresponding pressure field and the corrected velocity are represented in Fig. 1 (bottom), on the middle and on the right, respectively.

In the one-dimensional setting, existence of solutions can be obtained in various ways, as already mentioned ([15, 16, 17]). In higher dimension, system (8) (without the non-elastic collision law) can be obtained as a formal limit of compressible Euler equations with a singular pressure term (see [24]). Note also that solutions to a viscous version of (1) can be built (see [25, 26, 27]) as limits of solutions to compressible Navier-Stokes equations with a stiff pressure term.

Yet, up to our knowledge, there is no well-posedness result (in terms of existence or uniqueness) for the congested Euler system (8), for dimensions higher than 1.

We propose here a new time-discretization scheme for (8) in the spirit of the prediction-correction scheme used in the crowd motion case. This scheme will allow us to build sequences of densities and velocities, that may be expected to converge to weak solutions of our problem. Let us stress that we are not able to establish such a convergence, but we provide partial results that assert a certain consistency of the scheme with respect to the equations (see Section 2.2). Beside, a numerical scheme can be built on this time-splitting strategy, and we shall present preliminary results in Section 3.

Compared to the first order in time model, the present context of inertial particles raises two deep additional difficulties:

1. The velocity field is no longer prescribed as in the crowd motion case, it is attached to the mass and it is highly varying in time. In particular, it is not possible to control its regularity in space, so that the transport step in (7) may not be one-to-one, which means that particle trajectories cross each other. This is likely to lead to non-physical behaviour: particles crossing without seeing each other, or even artefactual energy increases during the subsequent projection phase. This calls for an additional step in the time-stepping procedure, by prescribing some sort of monotonicity in the transport phase.
2. For the very same reason (the velocity field is not prescribed once and for all), velocities have to be updated at the end of each time step. In particular, the effect of congestion (i.e. the projection phase) changes the velocity field and reduces energy, since we consider non-elastic collisions. This necessitates to follow the motion in a Lagrangian way during the whole scheme, i.e. to map the initial density to the final one respectfully of the actual motion of particles.

2 Time-stepping scheme

We first present here the issues raised by the attempt to propose a relevant time-stepping strategy for the congested pressureless Euler equations. We shall in particular explain, in a one-dimensional setting, how the two constraints (particles do not cross *and* the density remains below 1) can be accounted for in a mutually consistent way. We then present the time-stepping scheme in any space dimension, and we detail some of its properties.

2.1 Time discretization strategy

We first consider the microscopic model (3) in one dimension (aligned grains), assuming that the grain diameter is zero (which makes clear sense in the one-dimensional setting), and that no force is exerted. We assume that, at initial time, the ordering is consistent with the indexing:

$$q_i(0) \leq q_j(0) \quad \text{for} \quad 0 \leq i \leq j \leq N.$$

Since they do not leap over each other, the set of admissible configurations expresses that the order is preserved:

$$\tilde{K} = \{q \in \mathbb{R}^N,\ q_i \leq q_j \quad \forall i \leq j\},$$

and the set of feasible velocities follows

$$C_q = \{v \in \mathbb{R}^N,\ v_i \leq v_j \quad \text{whenever} \quad q_i = q_j\}.$$

The model of 1d granular flow with inelastic collisions may be phrased formally

$$\frac{dq}{dt} = u\ ,\quad u^+ = \mathbb{P}_{C_q}(u^-).$$

For this model, a numerical scheme and convergence results have been obtained in [28] and [19]. Let $\tau > 0$ be the time step and consider q^n, $v^n \in \mathbb{R}^n$ the position and velocity vectors at time $n\tau$. We ensure that the updated position vector $q^{n+1} = q^n + \tau u^n$ is admissible by prescribing

$$\forall i \leq j,\ \ q_i^n + \tau u_i^n \leq q_j^n + \tau u_j^n$$

and we call $C^\tau_{q^n}$ the corresponding set of velocities. The approximated solutions are built using the following scheme :

$$\begin{cases} u^{n+1} = \mathbb{P}_{C^\tau_{q^n}}(u^n); \\ q^{n+1} = q^n + \tau u^{n+1}. \end{cases} \tag{9}$$

Note that the conditions defining $C^\tau_{q^n}$ can be rewritten

$$\left(u_i^n - u_j^n\right) \cdot \left(q_i^n - q_j^n\right) \geq \frac{-1}{\tau} \left|q_i^n - q_j^n\right|^2. \tag{10}$$

There is an obvious link between this microscopic setting and the macroscopic system (1). Indeed, to any solution $(q(t), u(t))$ of the previous model, one can associate a solution to the macroscopic equation (1) considering the density $\rho_t = \sum_{i=1}^n \delta_{q_i(t)}$ and $\rho_t u_t = \sum_{i=1}^n u_i(t)\delta_{q_i(t)}$. It suggests a time-stepping scheme

to tackle the unconstrained macroscopic problem in one dimension, by simply requiring that trajectories do not cross during a time step τ, in the spirit of the strategy that is proposed in [11]. This scheme reads as follows: consider the density-velocity couple (ρ^n, u^n) at time step n, define the velocity $\tilde{u}^n$ as the projection of u^n on the cone of feasible velocities (macroscopic counterpart of (10))

$$C^\tau_{\rho^n} = \left\{ v \in L^2_{\rho^n} \ , \ \ (x-y)(v(x)-v(y)) \geq \frac{-1}{\tau}|x-y|^2 \text{ for } \rho^n \otimes \rho^n - a.e.(x,y) \right\},$$

and move ρ^n by $\mathrm{Id} + \tau\tilde{u}^n$ to obtain ρ^{n+1}. The new velocity u^{n+1} that is defined on the support of ρ^{n+1} is finally obtained by conservation of momentum between any y in the support of ρ^{n+1} and the set of its preimages $x \in (\mathrm{Id} + \tau\tilde{u}^n)^{-1}$.

Now consider the problem with congestion, i.e. the density is subject to remain below 1, it is natural to treat it in the spirit of Algorithm (7), that was dedicated to the first order in time model (crowd motion), by considering that the previous velocity u^n plays the role of the desired velocity. It consists in projecting the predicted measure (obtained according to the previous considerations) on the set of feasible densities (second step of (7)).

The drawback of this scheme is that the intermediate density obtained after handling the non-crossing of trajectories may contain a singular part, typically at points y that can be written $x + \tau\tilde{u}^n(x)$ for x running over a set with non zero ρ^n-measure. This feature would not be a problem if the pre-collisional velocities were prescribed, like in the crowd motion problem. But in the case of pressureless equation, it is necessary to build the new velocity field over the support of the new density. It requires to follow the motion of individual particles before and after the two sub-steps of the procedure. This is prevented by the presence of Dirac masses in the intermediate measure: they make it impossible to properly define a map between the previous density field and the next one, in a way that would respect the Lagrangian motion of particles.

For this reason, we propose to reinforce the non-crossing constraint by prescribing that trajectories do not cross in a strict sense, i.e. particles remain, during the whole time step, at a distance that is bounded from below. More precisely, consider two particles initially at x and y, with velocities v_x and v_y, respectively. We require that the moving particles remain at a distance that is larger than c times their initial distance, where $c \in (0,1)$ is a small parameter:

$$\begin{aligned} \langle x-y, (x+\tau v_x) - (y+\tau v_y) \rangle &\geq c\,|x-y|^2 \\ \iff \langle x-y, v_x - v_y \rangle &\geq \left(\frac{c-1}{\tau}\right)|x-y|^2. \end{aligned}$$

This constraint will be integrated in the process through the definition of the set of feasible velocities introduced in the next section (Eq. (12)). The positivity of c forces the intermediate density $\tilde{\rho}^{n+1}$ to remain bounded (see Lemma 2.2) and the transport $\mathrm{Id} + \tau\tilde{v}^n$ to be invertible. Thus, one can reconstruct the trajectory of particles from the density ρ^{n+1} to ρ^n with the composition of two Lagrangian transports.

The next section will detail the time-stepping scheme issued from the previous one-dimensional consideration. The approach we propose is far from being covered by a full convergence analysis. Yet, beyond the fact that very few methods exist to build solutions for the congested pressureless Euler equation in dimension $d \geq 2$, the approach is supported by the following properties, that are detailed in the next section:

1. The scheme is well-defined, in the sense that each time step defines in a unique way a new density, that verifies the congestion constraint, and an associated velocity field;
2. In a one-dimensional setting, in the case of an initial density that is a collection of saturated clusters (sum of characteristic functions of intervals), our scheme essentially behaves like the so-called sticky block approach, meaning that numerical solutions actually converge, in this setting, to solutions of the continuous problem (as proved in [16]);
3. In any dimension, the scheme conserves the momentum of material systems during collision. More precisely, for each material subsystem involved in a numerical collision, the momentum is conserved;
4. Since the approach is not based on a relaxation of the congestion constraint, it natively handles empty zones without difficulty, as confirmed by the numerical illustrations that are presented.

2.2 The scheme

Let $\Omega \subset \mathbb{R}^d$ be a bounded domain, we denote by $\mathcal{P}(\bar{\Omega})$ the space of probability measures on $\bar{\Omega}$. We shall assume in what follows that the domain is chosen sufficiently large, so that all considered densities are supported in it.

Let $\tau > 0$ be a time step, $\rho^n \in \mathcal{P}(\bar{\Omega})$ and $u^n \in L^2_{\rho^n}(\bar{\Omega})$ represent the density and velocity at time $n\tau$. The first step consists in projecting the current velocity field on the set of $\mathcal{M}^c_{\rho^n}$, to prevent particles from crossing. The density is then moved according to this projected velocity field, during τ. The obtained intermediate density is likely to violate the constraint. The third step consists in

projecting it (in the Wasserstein sense), on the feasible set K, to account for the saturation constraint. The final step consists in defining the new (post-collision) velocity, using the Lagrange map between the previous density and the new one.

For (ρ^n, u^n) given, the scheme reads:

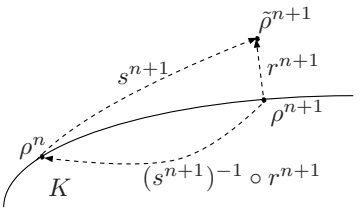

$$\begin{cases} \tilde u^n = \mathbb{P}_{\mathcal{M}^c_{\rho^n}}(u^n) \\ \tilde\rho^{n+1} = (\mathrm{Id} + \tau\tilde u^n)_{\#}\,\rho^n \\ \rho^{n+1} = \mathbb{P}^{\mathcal{W}_2}_K(\tilde\rho^{n+1}) \\ u^{n+1} = \dfrac{\mathrm{Id} - (s^{n+1})^{-1}\circ r^{n+1}}{\tau} \end{cases} \tag{11}$$

with

$$\mathcal{M}^c_{\rho^n} = \{v \in L^2_{\rho^n}(\bar\Omega)\,,\ \langle v(x) - v(y), x-y\rangle \geq \frac{c-1}{\tau}|x-y|^2\ \rho^n\otimes\rho^n - a.e.\},\ (12)$$

and $c \in (0,1)$ a small parameter. K is the space of all those probability measures supported in $\bar\Omega$ that admit a density less than 1. The mappings involved in the last step (reconstruction of the velocity) are

$$s^{n+1} = \mathrm{Id} + \tau\tilde u^n,$$

and r^{n+1}, that is the optimal transportation map between ρ^{n+1} and $\tilde\rho^{n+1}$.

Figure 2 illustrates how the time-stepping scheme treats a one-dimensionnal collision between two blocks. The figure reads from bottom to top. The first part of the scheme moves densities with the current velocity, while avoiding contact of pathlines (the velocity is projected on $\mathcal{M}^c_{\rho^n}$). This intermediate density violates the congestion constraint, and the second step is meant to enforce it, by projection of the density on K. The 3 circles on the figure correspond to successive positions of a physical particle during the scheme: initially at x, it is moved to y, and then to z by projection. For this very particle, the reconstruction of the after-collision velocity (at the new position z) gives $(z-x)/\tau$. As explained in the proof of Proposition 3, it may happen that a gap remains between the two blocks after this first partial treatment, in that case it may need two more time steps to fully handle the collision.

Let us start by establishing some basic properties pertaining to the proposed scheme. The first lemma asserts that the first step (projection on $\mathcal{M}^c_{\rho^n}$) is well-defined, and preserves the total momentum. In a second lemma, we show that the intermediate density $\tilde\rho^{n+1}$ is bounded. In the third one, we recall a known result concerning the projection on K.

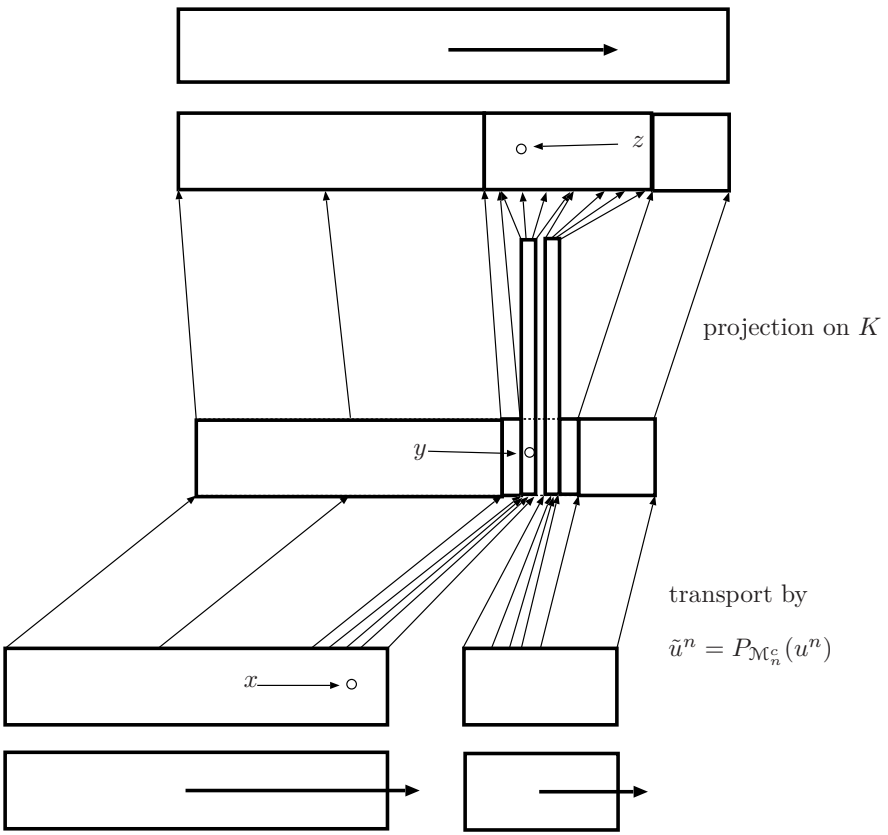

Fig. 2. Time stepping scheme for a 1d collision

Lemma 2.1. *Let $\rho \in \mathcal{P}(\bar{\Omega})$ and $u \in L^2_\rho(\bar{\Omega})$, then there exists a unique $\tilde{u} \in \mathcal{M}^c_\rho$ such that :*

$$\|u - v\|_{L^2_\rho(\bar{\Omega})} \geq \|u - \tilde{u}\|_{L^2_\rho(\bar{\Omega})}, \forall v \in L^2_\rho(\bar{\Omega}).$$

Moreover, we have the following properties :

(i) $\|\tilde{u}\|_{L^2_\rho(\bar{\Omega})} \leq \|u\|_{L^2_\rho(\bar{\Omega})}$;

(ii) $\displaystyle\int_{\bar{\Omega}} \tilde{u}(x) d\rho(x) = \int_{\bar{\Omega}} u(x) d\rho(x).$

Proof. Since $\mathcal{M}^c_\rho$ is a closed and convex set, the projection $\tilde{u} := \mathbb{P}_{\mathcal{M}^c_\rho}(u)$ is well-defined. Inequality (i) comes from the fact $\mathcal{M}^c_\rho$ is also a cone pointed at 0.

Let us prove now that the first step of the scheme does not change momentum (identity (ii)). If $u \in \mathcal{M}^c_\rho$, then $u + k$ is also in $\mathcal{M}^c_\rho$ for any k in $\mathbb{R}^d$. If $\tilde{u}$ is

the projection of u on $\mathcal{M}^c_\rho$, we have :

$$\|u-\tilde{u}\|^2_{L^2_\rho(\bar{\Omega})} \leq \|u-\tilde{u}-k\|^2_{L^2_\rho(\bar{\Omega})}$$

and thus :

$$\left\langle u-\tilde{u}, \frac{k}{|k|} \right\rangle_{L^2_\rho(\bar{\Omega})} \leq \frac{|k|}{2}.$$

Letting $|k|$ tend to 0 yields $\left\langle u-\tilde{u}, \frac{k}{|k|} \right\rangle_{L^2_\rho(\bar{\Omega})} \leq 0$, for all $k \in \mathbb{R}^d$ and consequently

$$\left\langle u-\tilde{u}, \frac{k}{|k|} \right\rangle_{L^2_\rho(\bar{\Omega})} = 0.$$

Consider the total momenta before and after the projection of velocities:

$$E_{tot} = \int_{\bar{\Omega}} u(x) d\rho(x) \quad \text{and} \quad \tilde{E}_{tot} = \int_{\bar{\Omega}} \tilde{u}(x) d\rho(x).$$

We have $\langle E_{tot}, k\rangle = \langle \tilde{E}_{tot}, k\rangle$ for all $k \in \mathbb{R}^d$ and finally $\tilde{E}_{tot} = E_{tot}$. □

Lemma 2.2. *Let $\tilde{\rho} := s_{\#}\rho = (Id + \tau\tilde{u})_{\#}\rho$, with $\rho \in L^\infty(\bar{\Omega})$, and $\tilde{u} \in \mathcal{M}^c_\rho$, we have :*

$$\|\tilde{\rho}\|_{L^\infty(\bar{\Omega})} \leq \frac{1}{c^d} \|\rho\|_{L^\infty(\bar{\Omega})}.$$

Proof. We consider here that $\tilde{u}$ is regular, and we refer to [29], Section 5.5, for the general case. Since $\tilde{u}$ is in $\mathcal{M}^c_\rho$, the eigenvalues of ∇s are larger than c and then $\det \nabla s$ is larger than c^d. Finally, since $\tilde{\rho} = \dfrac{\rho}{|\det \nabla s|} \circ s^{-1}$ we have

$$\|\tilde{\rho}\|_{L^\infty(\bar{\Omega})} = \left\| \frac{\rho}{|\det \nabla s|} \circ s^{-1} \right\|_{L^\infty(\bar{\Omega})} \leq \frac{1}{c^d} \left\| \rho \circ s^{-1} \right\|_{L^\infty(\bar{\Omega})} \leq \frac{1}{c^d} \|\rho\|_{L^\infty(\bar{\Omega})},$$

which ends the proof. □

The following lemma concerns the projection on K. It is proven in [21].

Lemma 2.3. *Let $\rho \in \mathcal{P}(\bar{\Omega})$. There exists a unique $\rho_K \in K$ such that*

$$\mathcal{W}_2(\rho,\mu) \geq \mathcal{W}_2(\rho,\rho_K), \forall \mu \in K,$$

and there exists $\pi \in \{p \in H^1 | \, p \geq 0, (1-\rho)p = 0\}$ such that

$$\rho = (Id + \nabla\pi)_{\#}\rho_K.$$

We may know prove that the scheme defines a unique density-velocity couple.

Proposition 1. *Let* $(\rho^n, u^n) \in K \times L^2_{\rho^n}(\bar{\Omega})$. *The scheme* (11) *defines a unique* $(\rho^{n+1}, u^{n+1}) \in K \times L^2_{\rho^{n+1}}(\bar{\Omega})$.

Proof. We can check that s^{n+1} is strictly monotone and consequently injective. We can define an inverse on $s^{n+1}(\mathrm{spt}(\rho^n)) = \mathrm{spt}(\tilde{\rho}^{n+1})$. Thanks to Lemma 2.3, we have existence and uniqueness of $r^{n+1} : \mathrm{spt}(\rho^{n+1}) \to \mathrm{spt}(\tilde{\rho}^{n+1})$ and consequently the uniqueness of u^{n+1} and ρ^{n+1}. Moreover, we have

$$
\begin{aligned}
&\int_{\bar{\Omega}} (u^{n+1}(x))^2 \rho^{n+1}(x)dx \\
= &\int_{\bar{\Omega}} \left(\frac{x - (s^{n+1})^{-1} \circ r^{n+1}(x)}{\tau} \right)^2 \rho^{n+1}(x)dx \\
= &\int_{\bar{\Omega}} \left(\frac{(r^{n+1})^{-1}(x) - (s^{n+1})^{-1}(x)}{\tau} \right)^2 \tilde{\rho}^{n+1}(x)dx \\
\leq &\ 2 \int_{\bar{\Omega}} \left[\left(\frac{(r^{n+1})^{-1}(x) - x}{\tau} \right)^2 + \left(\frac{x - (s^{n+1})^{-1}(x)}{\tau} \right)^2 \right] \tilde{\rho}^{n+1}(x)dx \\
\leq &\ 2 \int_{\bar{\Omega}} \left(\frac{x - r^{n+1}(x)}{\tau} \right)^2 \rho^{n+1}(x)dx + 2 \int_{\bar{\Omega}} \left(\frac{s^{n+1}(x) - x}{\tau} \right)^2 \rho^n(x)dx \\
\leq &\ 2 \int_{\bar{\Omega}} (\nabla \pi^{n+1}(x))^2 \rho^{n+1}(x)dx + 2 \int_{\bar{\Omega}} \tilde{u}^n(x)^2 \rho^n(x)dx \\
\leq &\ 4 \int_{\bar{\Omega}} u^n(x)^2 \rho^n(x)dx
\end{aligned}
$$

since

$$
\int_{\bar{\Omega}} \left(\nabla \pi^{n+1}(x) \right)^2 \rho^{n+1}(x)dx = \mathcal{W}_2(\rho^{n+1}, \tilde{\rho}^{n+1}) \leq \mathcal{W}_2(\rho^n, \tilde{\rho}^{n+1})
$$

and

$$
\mathcal{W}_2(\rho^n, \tilde{\rho}^{n+1}) \leq \int_{\bar{\Omega}} u^n(x)^2 \rho^n(x)dx,
$$

which ends the proof. □

Proposition 2. *Total mass and momentum are conserved by the scheme* (11).

Proof. Conservation of mass is inherent to the approach, which is a succession of transports and projections in the Wasserstein sense. As for the momentum, we have already seen that $\int_{\bar\Omega} E^n(x)dx = \int_{\bar\Omega} \tilde E^n(x)dx$, where $\tilde E^n = \rho^n \tilde{v^n}$.

$$\begin{aligned}
&\int_{\bar\Omega} \tilde E^n(x)\phi(x)dx \\
= &\int_{\bar\Omega} \rho^n(x)\tilde u^n(x)\phi(x)dx \\
= &\int_{\bar\Omega} ((s^{n+1})^{-1}\circ r^{n+1})_\# \rho^{n+1}(x)\tilde u^n(x)\phi(x)dx \\
= &\int_{\bar\Omega} ((s^{n+1})^{-1}\circ r^{n+1})_\# \rho^{n+1}(x)(\frac{s^{n+1}(x)-x}{\tau})\phi(x)dx \\
= &\int_{\bar\Omega} \rho^{n+1}(x)(\frac{r^{n+1}-(s^{n+1})^{-1}\circ r^{n+1}}{\tau})\phi((s^{n+1})^{-1}\circ r^{n+1}(x))dx \\
= &\int_{\bar\Omega} \rho^{n+1}(x)(\nabla\pi^{n+1}+u^{n+1})\phi((s^{n+1})^{-1}\circ r^{n+1}(x))dx
\end{aligned}$$

So $\tilde E^n_\tau = (s^{n+1})^{-1}\circ r^{n+1})_\#(\rho^{n+1}\nabla\pi^{n+1} + E^{n+1})$ and consequently :

$$\begin{aligned}
\int_{\bar\Omega} \tilde E^n(x)dx &= \int_{\bar\Omega} \rho^{n+1}(x)(\nabla\pi^{n+1}(x)+u^{n+1}(x))dx \\
&= \int_{\bar\Omega} \rho^{n+1}(x)\nabla\pi^{n+1}(x) + \int_{\bar\Omega} \rho^{n+1}(x)u^{n+1}(x)dx \\
&= \int_{\bar\Omega} E^{n+1}(x)dx.
\end{aligned}$$

□

Remark 2. *A direct consequence of the previous proposition is that the center of mass moves at a constant velocity*

$$U = \frac{\int_{\bar\Omega} u^n(x)\rho^n(x)dx}{\int_{\bar\Omega}\rho^n(x)dx}.$$

The next proposition pertains to the one-dimensional setting. We consider the exact solution that corresponds to the collision of two saturated blocks. We establish that, except for the few times steps (no more than 3) that are needed

to handle the collision at the discrete level, the discretization scheme recovers the exact solution.

Proposition 3. *Let ρ_t be the density representing two blocks colliding at time t_0 and $\eta > 0$. If $c \leq \sqrt{2} - 1$ then there exists $\tau_o > 0$ such that for all time step $\tau \leq \tau_o$ the solution given by the scheme is exact, for all step $n \in \{n \in \mathbb{N},\, n\tau \notin [t_0 - \eta, t_0 + \eta]\}$.*

Proof. Let us start by two basic remarks. Firstly, from remark 2, the scheme computes in an exact way the motion of the mass center. Secondly, an isolated block moving at uniform velocity is preserved by the scheme (blocks stay blocks). As a consequence, we just have to check that the scheme makes the blocks stick together in a finite number of steps (no more than 3, as we shall see).

Let $\Delta U^n \geq 0$ be the velocity difference between the two blocks at time $n\tau$ and e^n their distance. One can check that the updated velocity difference ΔU^{n+1} is equal to $\frac{e^n - e^{n+1}}{\tau}$. The velocity field u^n remains in $\mathcal{M}^c_{\rho^n}$ if and only if the constraint is verified in the ends of blocks, so that

$$\begin{aligned} & \Delta U^n(-e^n) \geq \tfrac{c-1}{\tau}(e^n)^2 \\ \Leftrightarrow \qquad & \tau \Delta U^n \leq (1-c)e^n \end{aligned}$$

Now, if $\tau \Delta U^n > (1-c)e^n$ and if the length of the smaller block L is sufficiently large (take τ such that $L \geq 2\tau ||v||_\infty$) the density $\tilde{\rho}^{n+1}$ exceeds the congestion constraint (see Figure 2) over two blocks of total size $\frac{c\tau\Delta U^n}{1-c} - ce^n$. In this case, the mass M projected in the gap between the two blocks is larger than the half of over-congested mass,

$$M \geq \frac{1}{2}\left(\frac{1}{c} - 1\right)\left(\frac{c\tau\Delta U^n}{1-c} - ce^n\right) \geq \frac{1}{2}(\tau\Delta U^n + (c-1)e^n).$$

Two cases have to be considered. If $\tau\Delta U^n \geq (1+c)e^n$, the mass M is larger than the mass necessary to refill the gap, this implies $e^{n+1} = 0$ and $\tau\Delta U^{n+1} = e^n$. The following step allows blocks to have the same velocity, $e^{n+2} = 0$ and $\Delta U^{n+2} = 0$. So, the scheme handles the collision with 2 steps.
Now if $\tau\Delta U^n \in ((1-c)e^n, (1+c)e^n)$, the projection on the set of feasible velocities imposes that $\tilde{e}^{n+1} = ce^n$ (the distance between the ends of blocks is exactly c times the previous one), then $e^{n+1} \leq ce^n$ and consequently

$$\tau\Delta U^{n+1} = e^n - e^{n+1} \geq (1-c)e^n.$$

Thus,

$$(1+c)e^{n+1} \leq (1+c)ce^n \leq (1-c)e^n \leq \tau\Delta U^{n+1}$$

since $c \leq \sqrt{2}-1$, conditions of the first case are obtained, the scheme handles the collision with 3 steps.

Finally, taking $\tau_o = \min\{\frac{L}{2\|v\|_\infty}, \frac{2\eta}{5}\}$ allows us to prove the property. □

3 Numerical illustrations

We briefly describe here a space discretization strategy that can be carried out to perfom actual simulations, and we present some numerical tests to illustrate the behavior of the numerical scheme in various situations.

3.1 Space discretization scheme

We take $\bar{\Omega} = [0,1]^2$ and we discretize the domain in a collection of cells $(C_i)_{i\in I}$ with a uniform size $h \times h$ and the center located at x_i. The quantities used previously are approximated by constant functions in each cell :

$$f \approx \sum_{i\in I} f(x_i)\mathbb{1}_{C_i} := \sum_{i\in I} f_i \mathbb{1}_{C_i},$$

and we denote by X_h^α the corresponding space ($\alpha = 1$ for a scalar field, $\alpha = 2$ for a vector field). From now on, we will assimilate f to the vector $(f_i) \in (\mathbb{R}^d)^I$.We denote by I_ρ the set of indices corresponding to non-zero values of the ρ_i's: $I_\rho = \{i \in I \,|\, \rho_i > 0\}$. We may now describe the 4 steps of the numerical scheme.

Suppose that we have $(\rho^n, v^n) \in X_h^1 \times X_h^2$.
Step 1 : We replace $\mathcal{M}_n^c$ by the space of functions v in X_h^2 such that

$$\forall i,j \in I_{\rho^n},\ \langle v_i - v_j, x_i - x_j\rangle \geq \left(\frac{c-1}{\tau}\right)|x_i - x_j|^2.$$

The projection can be formulated in a saddle-point form: Consider the function $F_{ij} := v \to \langle v_i - v_j, x_i - x_j\rangle - \left(\frac{c-1}{\tau}\right)|x_i - x_j|^2$, the projection onto this space is defined as

$$\tilde{v}^n = \underset{\tilde{v}\in\mathbb{R}^I}{\operatorname{argmin}} \left\{ \sup_{\lambda_{ij}\in\mathbb{R}_+^{I^2}} \left(\|\tilde{v} - v^n\|_{\ell^2_{\rho^n}} - \sum_{i,j\in(I_{\rho^n})^2} \lambda_{ij} F_{ij}(v^n) \right) \right\}.$$

Step 2 : We approximate the transport step by a projected Lagrangian scheme (see Remark 3):

$$\tilde{\rho}^{n+1} := (\mathrm{Id} + \tau\tilde{v}^n)_{\#}\rho^n \quad \approx \quad \sum_{i\in I}\left(\int_{C_i}(\mathrm{Id}+\tau\tilde{v}^n)_{\#}\rho^n(x)dx\right)\mathbb{1}_{C_i},$$

$$\tilde{E}^{n+1} := (\mathrm{Id} + \tau\tilde{v}^n)_{\#}E^n \quad \approx \quad \sum_{i\in I}\left(\int_{C_i}(\mathrm{Id}+\tau\tilde{v}^n)_{\#}E^n(x)dx\right)\mathbb{1}_{C_i}.$$

Step 3 : In order to project on K, we define the discrete transport plan as the minimizer of a discrete counterpart of the transport cost, among all those plans $\zeta = (\zeta_{ij})_{i,j\in I}$ with $\tilde{\rho}^{n+1}$ as first marginal, and second marginal in K. The cost is defined as

$$C(\zeta) = \sum_{i\in I_{\tilde{\rho}^{n+1}}}\sum_{j\in I}\beta_{ij},$$

where the cell-to-cell costs β_{ij} are defined (see Remark 4) by

$$\beta_{ij} = \begin{cases} \dfrac{\zeta_{ij}^2}{\tilde{\rho}_i^{n+1}}|x_i - x_j|^2 & \text{if } C_i \text{ is a neighbor of } C_j \\ +\infty & \text{otherwise} \end{cases} \tag{13}$$

where cells are considered neighbors if they share an edge or a vertex. The infinite cost for non-neighboring cells prevents the transport from leaping over adjacent cells. This choice is consistent with the fact that very small time steps are used in the presented illustrations.

Step 4 : We reconstruct the velocity by

$$E_j^{n+1} = \sum_{i\in I_{\tilde{\rho}^{n+1}}}\zeta_{ij}\left(\frac{\tilde{E}_i^{n+1}}{\tilde{\rho}_i^{n+1}} + \left(\frac{x_j - x_i}{\tau}\right)\right), \quad u_j^{n+1} = E_j^{n+1}/\rho_j^{n+1}.$$

Remark 3. *Note that the space X_h is not stable by the transportation step. If $\rho \in X_h^1$, then $(Id+\tau v)_{\#}\rho$ is a piecewise constant function that is not, in general, in X_h^1. A function in X_h^1 is obtained by ℓ^2 projection.*

Remark 4. *The step 3 is undoubtedly the most problematic one. A natural counterpart of the continuous projection problem would consist in minimizing*

$$\sum_{i,j}\zeta_{ij}|x_i - x_j|^2$$

over all those discrete transport plans (ζ_{ij}) *with* $\tilde{\rho}^{n+1}$ *as first marginal, and such that the second marginal belongs to* K*. Yet, this straight discretization of the transport cost does not lead to a satisfying approximation of the projection. This feature is related to the numerical diffusion that is inherent to the space discretization of the Finite Volume type that we chose. This delicate issue will be addressed in a forthcoming paper. Let us simply say here that, if one considers the JKO scheme applied to the gradient flow that corresponds to transport at constant velocity, such a discretization leads to an untenable behaviour. For small time steps, the discretized JKO scheme is static, i.e. the density is not transported. It comes from the fact that, because of numerical diffusion, the expression above highly overestimates the cost of the displacement from a cell to its neighbor, so that immobility is cheaper than cell-to-cell motion. This locking phenomenon can be avoided by changing the cost for short displacements. More precisely, it can be checked in the transport case that changing the cost into*

$$\frac{\zeta_{ij}^2}{\tilde{\rho}_i^{n+1}}|x_i - x_j|^2$$

makes it possible to recover the classical upwind scheme in the one-dimensional case. This explains the choice of the cost of transport between neighboring cells that appears in (13)*.*

3.2 Numerical tests

In this part, we illustrate our comments by comparing numerical solutions computed by the SCoPI software for the granular model (see [30, 31, 32] for details on the algorithm) with the solutions computed by our algorithm for the scheme described above. This comparison is not intended to rigorously validate the approach in any way, since the two models are different (see next section), but it asserts a satisfactory behaviour of the macroscopic model to mimic the motion of many-body suspensions. In the microscopic examples we take the number of particles (with a radius of r given below) that corresponds to the density of the macroscopic model.

First numerical example :
In this case, a small cloud of particles (on the left) is set at uniform (rightward) velocity toward another cloud of particles initially at rest.
Macroscopic model :

- $\bar{\Omega} = [-40, 40]^2$, $h = 0.3$, $\tau = 0.0150$;
- $\rho^0 = 0.2\mathbb{1}_{x^2+y^2<25^2} + 0.2\mathbb{1}_{(x+31)^2+y^2<5^2}$;

- $E^0 = 2\mathbb{1}_{(x+31)^2+y^2<5^2}$.

Microscopic model :
- $\bar{\Omega} = [-40, 40]^2$, $\tau = 0.03$, $r = 0.1$;
- 500 particules in $\{(x+31)^2+y^2 < 5^2\}$ at velocity $(10, 0)$ and 12500 particules in $\{x^2 + y^2 < 25^2\}$ at velocity $(0, 0)$.

Second numerical example :
In this second situations, two square clouds of particles are thrown against each other.
Macroscopic model :
- $\bar{\Omega} = [-40, 40]^2$, $h = 0.3$, $\tau = 0.0075$;
- $\rho^0 = 0.5\mathbb{1}_{[0.5,20.5]\times[-10,10]} + 0.5\mathbb{1}_{[-20.5,-0.5]\times[-10,10]}$;
- $E^0 = -5\mathbb{1}_{[0.5,20.5]\times[-10,10]} + 5\mathbb{1}_{[-20.5,-0.5]\times[-10,10]}$.

Microscopic model :
- $\bar{\Omega} = [-40, 40]^2$, $\tau = 0.003$, $r = 0.1$;
- 5220 particles in $[0.5, 20.5] \times [-10, 10]$ at velocities (-10,0) and 5220 particles in $[-20.5, -0.5] \times [-10, 10]$ at velocities (10,0).

Figures 3 and 4 present the evolution of the macroscopic density (left), and the suspension of rigid grains (right), for the first test case. Figures 5 and 6 correspond to the second test case. In both examples, the shapes of the saturated zone that is induced by the collision of clouds present similar patterns. Note that symmetry-breaking seems to occur in the microscopic case. It is due to the fact that the grains are randomly distributed on the support of each cloud, so that the initial condition itself is not symmetric.

4 Conclusive remarks

Let us first stress that the macroscopic model that we propose cannot be obtained as a limit, even formally, of the hard sphere microscopic model. We refer to [20] for a detailed discussion on these delicate micro-macro issues. The microscopic granular arrangements of rigid spheres (or discs, for the two-dimensionnal setting) induce non local effects that cannot be captured by the crude macroscopic description that we proposed. Even the very notion of maximal density

does not have a clear meaning in the microscopic setting, especially in two dimensions: it depends on the local structure of grains.

Let us also mention that the macroscopic model can be extended, at least formally, to more general collision laws (see Remark 1 for the microscopic setting), i.e. with a restitution coefficient $e \in (0,1]$. It is a straight translation of the microscopic collision (4). Indeed, the dual cone of $C_K(\rho)$ (defined by (5)) is the outward normal cone

$$N_K(\rho) = \left\{ \nabla q \ , \ \ q \in H^1 \ , \ \ q \geq 0 \ , \ \ q(1-\rho) = 0 \right\}$$

which leads to the following macroscopic collision law

$$u^+ = u^- - (1+e) P_{N_K(\rho)} u^- .$$

The projection on $N_K(\rho)$ is obviously well-defined, since it is a closed convex cone. Yet, although the model seems to make clear sense, and at least formally determines the evolution of the system, very deep stability issues can be expected, even in the one-dimensional setting. Let us consider the case of two identical blocks colliding with opposite velocities, in 1d (see Fig. 1, top). With $e = 1$ (pure elastic collision), the expected solution can be recovered: the after-collisional velocities are simply the opposite velocities (pure bouncing between blocks). Now consider that the right hand side block, considered as $\mathbb{1}_{(0,1)}$ is replaced by the sum of $\mathbb{1}_{(0,a)}$ and $\mathbb{1}_{(a+\varepsilon,1+\varepsilon)}$, for a fixed $a \in (0,1)$. The behavior can be computed explicitely, and it is highly different from the previous situation (the sub-block at the right hand side will be pushed away at a higher velocity), for arbitrary small values of ε, which leaves little hope that the evolution may depend smoothly on initial conditions.

References

[1] F. Bouchut. On zero pressure gas dynamics. *Advances in kinetic theory and computing*, 22:171–190, 1994.

[2] Y. Brenier. Minimal geodesics on groups of volume preserving maps and generalized solutions of the Euler equations. *Communications on pure and applied mathematics*, 52(4):411–452, 1999.

[3] E. Grenier. Existence globale pour le systeme des gaz sans pression. *Comptes rendus de l'Académie des sciences. Série 1, Mathématique*, 321(2):171–174, 1995.

[4] W. E, Y.G. Rykov, and Ya.G. Sinai. Generalized variational principles, global weak solutions and behavior with random initial data for systems of conservation laws arising in adhesion particle dynamics. *Communications in mathematical physics*, 177(2):349–380, 1996.

[5] Ya. B. Zeldovich. Gravitational instability: An approximate theory for large density perturbations. *Astronomy and astrophysics*, 5:84–89, 1970.

[6] Y. Brenier and E. Grenier. Sticky particles and scalar conservation laws. *SIAM journal on numerical analysis*, 35(6):2317–2328, 1998.

[7] T. Nguyen and A. Tudorascu. Pressureless Euler/Euler-Poisson systems via adhesion dynamics and scalar conservation laws. *SIAM Journal on Mathematical Analysis*, 40(2):754–775, 2008.

[8] F. Huang and Z. Wang. Well Posedness for Pressureless Flow. *Communications in mathematical physics*, 222:117–146, 2001.

[9] L. Natile and G. Savaré. A Wasserstein approach to the one-dimensional sticky particle system. *SIAM Journal on Mathematical Analysis*, 41(4):1340–1365, 2009.

[10] F. Cavalletti, M. Sedjro, and M. Westdickenberg. A Simple Proof of Global Existence for the 1d Pressureless Gas Dynamics Equations. *SIAM Journal on Mathematical Analysis*, 47(1):66–79, 2015.

[11] F. Cavalletti, M. Sedjro, and M. Westdickenberg. A time discretization for the pressureless gas dynamics equations. *arXiv preprint arXiv:1411.1012*, 2014.

[12] A.N. Sobolevskii. The small viscosity method for a one-dimensional system of equations of gas dynamic type without pressure. *Dokl. Akad. Nauk*, 356:310–312, 1997.

[13] L. Boudin. A solution with bounded expansion rate to the model of viscous pressureless gases. *SIAM Journal on Mathematical Analysis*, 32(1):172–193, 2000.

[14] G. Wolansky. Dynamics of a system of sticky particles of finite size on the line. *Nonlinearity*, 20:2175–2189, 2007.

[15] F. Bouchut, Y. Brenier, J. Cortes, and J.-F. Ripoll. A Hierarchy of Models for Two-Phase Flows. *Journal of Nonlinear Science*, 10(6):639–660, December 2000.

[16] F. Berthelin. Existence and weak stability for a pressureless model with unilateral constraint. *Mathematical Models and Methods in Applied Sciences*, 12(02):249–272, 2002.

[17] F. Berthelin, P. Degond, M. Delitala, and M. Rascle. A model for the formation and evolution of traffic jams. *Archive for Rational Mechanics and Analysis*, 187(2):185–220, 2008.

[18] P. Ballard. The dynamics of discrete mechanical systems with perfect unilateral constraints. *Archive for Rational Mechanics and Analysis*, 154(3):199–274, 2000.

[19] B. Maury. A time-stepping scheme for inelastic collisions. *Numerische Mathematik*, 102(4):649–679, 2006.

[20] B. Maury, A. Roudneff-Chupin, F. Santambrogio, and J. Venel. Handling congestion in crowd motion modeling. *arXiv preprint arXiv:1101.4102*, 2011.

[21] B. Maury, A. Roudneff-Chupin, and F. Santambrogio. A macroscopic crowd motion model of gradient flow type. *Mathematical Models and Methods in Applied Sciences*, 20(10):1787–1821, 2010.

[22] J.J. Moreau. Evolution problem associated with a moving convex set in a hilbert space. *J. Differential Equations*, 26:346–374, 1977.

[23] B. Maury and J. Venel. A discrete contact model for crowd motion. *ESAIM Mathematical Modelling and Numerical Analysis*, 45:145–168, 2011.

[24] P. Degond, J.Hua, and L. Navoret. Numerical simulations of the Euler system with congestion constraint. *Journal of Computational Physics*, 230(22):8057–8088, 2011.

[25] P.-L. Lions and N. Masmoudi. On a free boundary barotropic model. In *Annales de l'IHP Analyse non linéaire*, volume 16, pages 373–410, 1999.

[26] D. Bresch, Charlotte Perrin, and E. Zatorska. Singular limit of a Navier–Stokes system leading to a free/congested zones two-phase model. *Comptes Rendus Mathematique*, 352(9):685–690, 2014.

[27] C. Perrin and E. Zatorska. Free/Congested Two-Phase Model from Weak Solutions to Multi-Dimensional Compressible Navier-Stokes Equations. *arXiv preprint arXiv:1410.0498*, 2014.

[28] F. Bernicot and A. Lefebvre-Lepot. Existence results for non smooth second-order differential inclusions, convergence result for a numerical scheme and application to the modeling of inelastic collisions. *Confluentes Mathematici*, 2(04):445–471, 2010.

[29] L. Ambrosio, N.Gigli, and G. Savaré. *Gradient flows: in metric spaces and in the space of probability measures*. Springer Science & Business Media, 2006.

[30] B. Maury. A time-stepping scheme for inelastic collisions. *Numerische Mathematik*, 102(4):649–679, February 2006.

[31] S. Faure and B. Maury. Crowd motion from the granular standpoint. *Mathematical Models and Methods in Applied Sciences*, 25(3):463–493, 2015.

[32] A. Lefebvre. Numerical simulation of gluey particles. *M2AN*, 43:53–80, 2009.

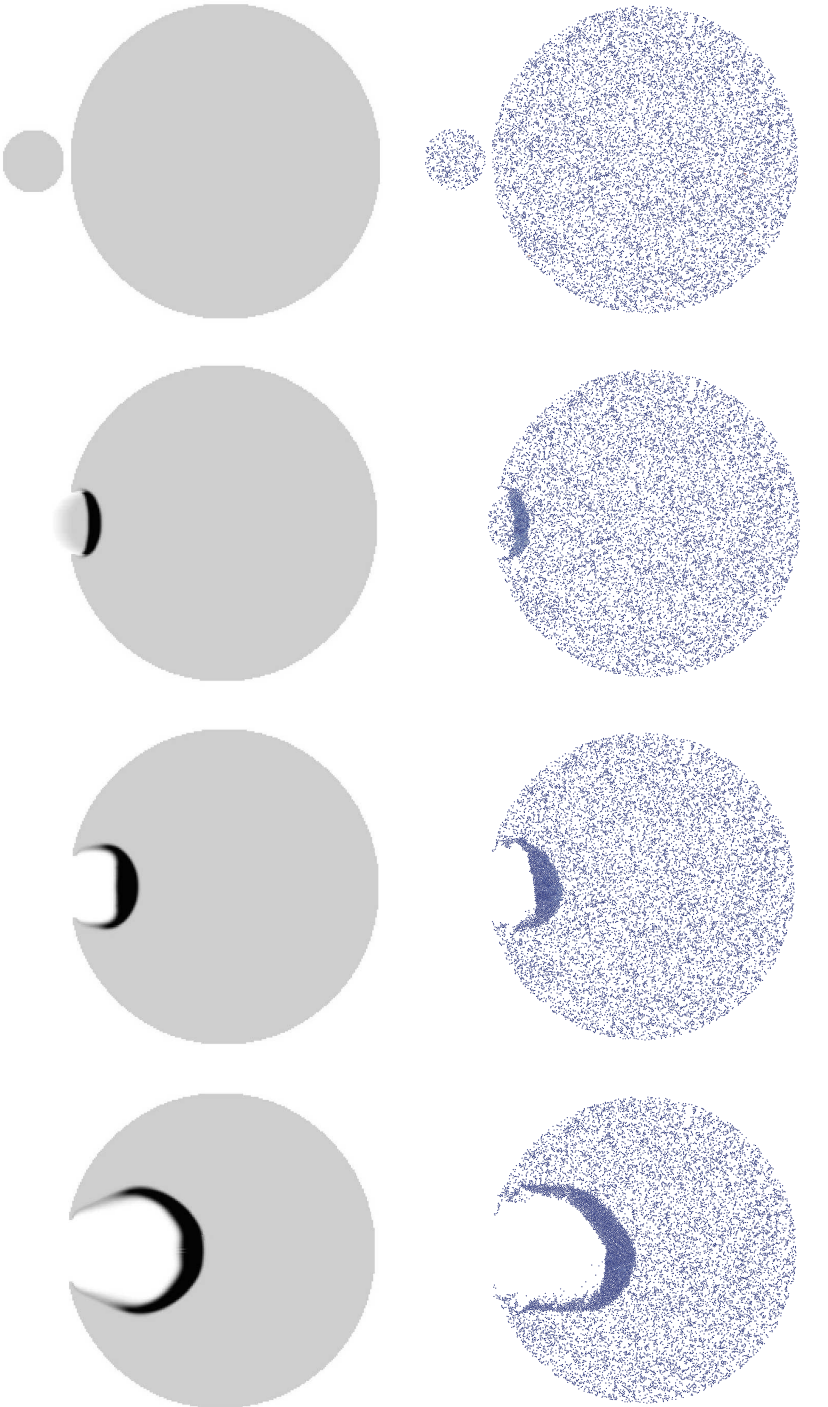

Fig. 3. First example at times 0, 1, 2 and 5.

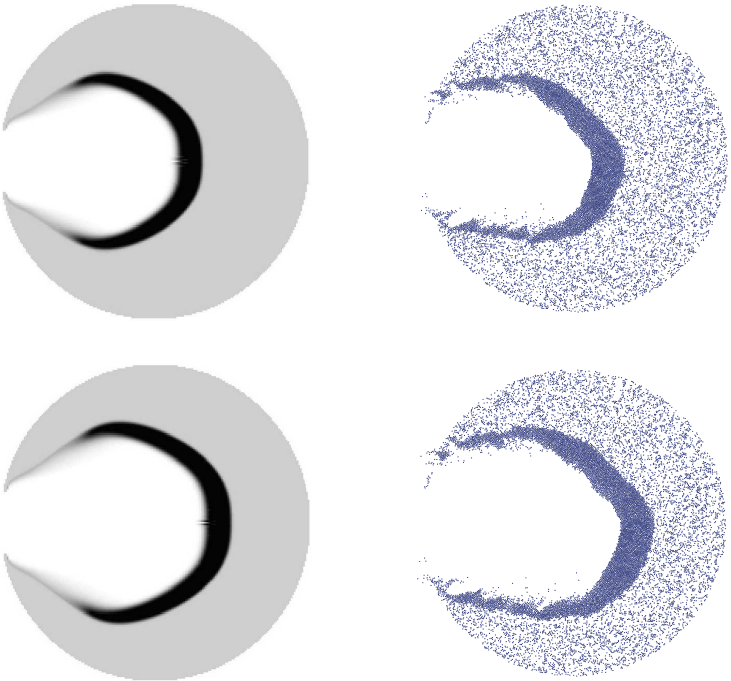

Fig. 4. First example at times 10 and 12.

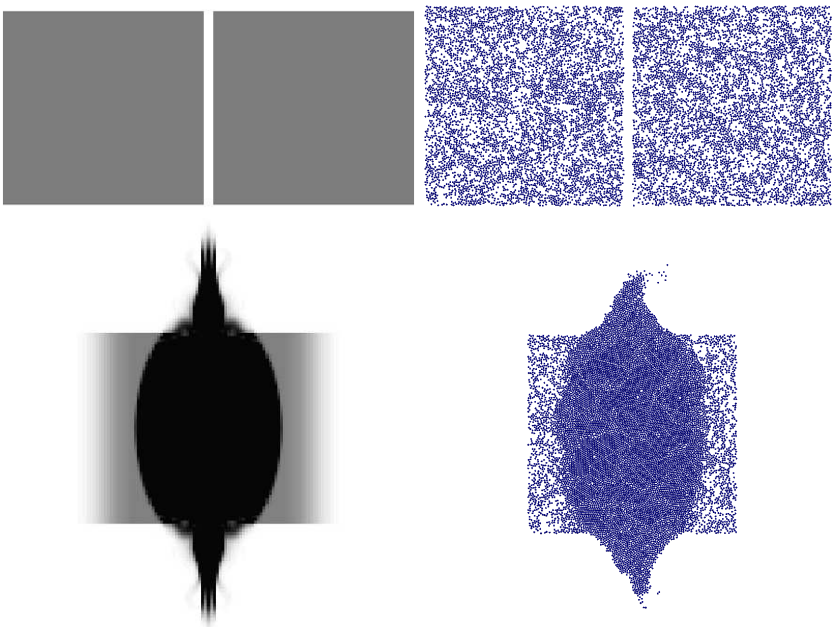

Fig. 5. Second example at times 0 and 1.

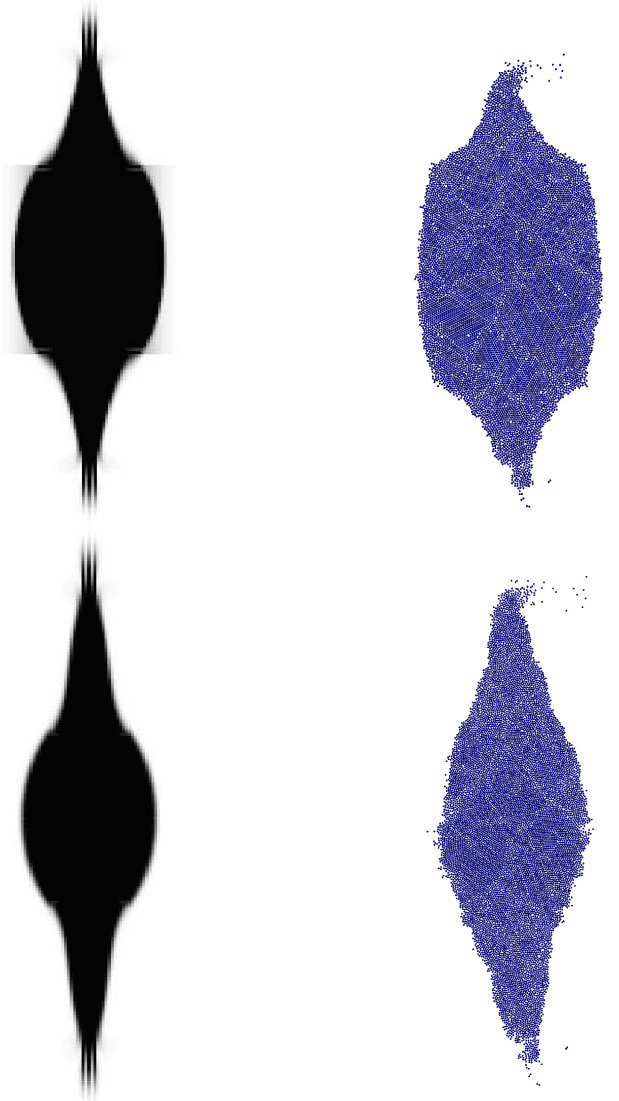

Fig. 6. Second example at times 1.5 and 2.